Size effect of gold nanoparticles on optical and electrical properties of plasmonic silicon solar cell

J. Gulomov [1], R. Aliev [1], I. Gulomova [1]
[1] Andijan State University, 170316, Andijan, Uzbekistan, Universitet str. 129

Abstract

One of important tasks of the day is increasing the efficiency and decreasing the cost of the silicon solar cells. There is method of introducing of metal nanoparticles into solar cells to improve its absorption and reduce transmission as well as reflection coefficients. When metal nanoparticles are introduced into silicon solar cell, nanoplasmonic effect will occur. Nanoplasmonic effect lead to modification of light spectrum and generation of extra hot electrons. Nanoplasmonic effect strongly depends on size of nanoparticles. Therefore, in this paper, effect of gold nanoparticles size on properties of silicon solar cell has been studied by using simulation. Gold nanoparticles with sizes of 4 nm, 6 nm, 9 nm, 11 nm and 21 nm have been input into emitter region of silicon solar cell in order to use both of nanoplasmonic-electric and nanoplasmonic-optic effects for enhancing efficiency of silicon solar cell. Open circuit voltage didn't change when size of nanoparticles has been changed from 4 nm to 11 nm. It dropped by 0.017 V when size of nanoparticles was 21 nm. Short circuit current has been maximum 6.7 mA/cm^2 at nanoparticle size of 11 nm and minimum 3.1 mA/cm^2 at nanoparticle size of 21 nm. It has been found from obtained results that gold nanoparticle with size of 11 nm affected significantly on properties of silicon solar cell. Besides, thickness of silicon solar cell can be decreased without dropping of efficiency by introducing gold nanoparticles. Because, main part of photons is absorbed near to metal nanoparticles inputted region.

Keywords: silicon, nanoplasmonics, nanoparticle, solar cell, simulation, gold.

Citation: Gulomov J, Aliev R, Gulomova I. Size effect of gold nanoparticles on optical and electrical properties of plasmonic silicon solar cell. Computer Optics 2022; 46(5): 733-740. DOI: 10.18287/2412-6179-CO-1089.

Acknowledgements: This work was supported by the Fundamental Research Project of Ministry of Innovative Development of the Republic of Uzbekistan (Project No. FZ-2020092973).

Introduction

Mainly, solar cells are utilized to convert solar energy to electricity. In industry, 96 % of solar cells are made from silicon [1] and therefore we focus on improving the efficiency and reducing the cost of silicon solar cells. Silicon is indirect band gap semiconductor and its band gap energy equals to 1.12 eV [2]. There are two main losses in solar cells which are optical and electrical losses. Optical loss includes especially spectral mismatch, reflection and transmission [3]. Silicon effectively absorbs light in visible range of spectrum [4]. Due to energy of light in infra-red spectrum being smaller than band gap energy of silicon, they aren't absorbed in silicon. If the photon energy equals to band gap energy, it is absorbed and creates electron-hole pair. If photon energy is greater than band gap energy, part of its energy, which is equaled to band gap energy, is expended to create electron-hole pair and rest of its energy is converted to thermal energy as phonons [5]. Because of ultraviolet light energy being high, it is mainly absorbed surface of silicon solar cell and creates electron-hole pair. But, as result of surface of silicon solar cell being more active, surface recombination rate increase. Hence, generated electron-hole pairs cannot reach to the contacts [6]. For overcoming this problem, the front surface of silicon solar cell is covered with luminescent materials that can lower photon energy [7]. Luminescent materials are divided into two groups that are down-shifting and up-conversion [8]. Luminescent downshifting materials absorb high energy photon then emits two low energy photons [9]. Luminescent up-conversion materials absorb two low energy photons then emit a high energy photon [10]. 30 % of incident light rays on surface of silicon solar cell are reflected owing to refractive index of silicon being 3.4 [11]. Surface of silicon solar cell is covered with 75 nm SiN_x [12] or 100 nm SiO_2 [13] to reduce the reflection coefficient and surface recombination rate as they have property of passivation the surface of silicon. Relying on the gradient refractive index law, multilayer optical systems also are utilized [14]. Besides, surface of silicon solar cell should be covered with upright pyramidal textures, according to mathematical studies, angle of pyramid base should be 73.12^0 or according to TCAD simulation results, angle of pyramid base should be 70.4^0 [15]. Other way to improve optical properties of silicon solar cell is forming the nanoholes and nanopillars on the surface of silicon solar cell [16]. By creating silicon/perovskite tandem structures, stability and efficiency of solar cell was increased because silicon solar cell has low efficiency and perovskite

solar cell has high degradation [17]. Nanocrystalline SiO_x can improve effective surface passivation and efficiency of silicon solar cell [18]. Covering with porous silicon on the frontal surface of silicon solar cell can help to increase its efficiency by improving optical properties [19]. There are some electrical losses such as recombination and parasitic resistivity in the silicon solar cell. Percentage of radiative recombination is in the range of 0 – 3 % owing to silicon is indirect band gap semiconductor [20]. Auger [21] and Shokley-Read-Hall (SRH) [22] recombination rates strongly depend on doping concentration. For instance, if 1e17 cm^{-3} phosphorous atoms and 1e15 cm^{-3} Bor atoms are doped respectively into emitter and base of silicon solar cell, in emitter region, percentages of Auger and SRH recombination will be 66 % and 32 % respectively, as well as in base region, SRH recombination will be dominant with 99.7 %. Another method to enhance the optical properties of solar cells is introducing metal nanoparticles into optical layers of solar cells. When light falls on the metal nanoparticle, the nanoplasmonic-electric and nanoplasmonic-optic effects occur [23]. First time, nanoplasmonic effect was observed in the Noble nanoparticles [24]. Nowadays, Au, Ag, Cu and Pt nanoparticles are widely used to form nanoplasmonic effect in solar cells [25]. Nanoparticles can be utilized for various purposes depend on their shapes. For example, using the metal nanoparticles with spherical shape for photovoltaic devices and cylindrical shape for thermoelectric devices gives good results [26]. Besides nanoparticles are used to increase performance of other optoelectronic devices such as nano-lasers [27] and sensors [28].

In nanoplasmonic effect when the light falls on the metal nanoparticle, free electrons on the surface of metal nanoparticle oscillate harmonically. The free electrons emit electromagnetic wave during oscillation. Thus, firstly, nanoparticles can modify the light wavelength by absorbing and emitting. Secondly, if incident photon frequency equals to oscillation frequency of free electrons, the resonance phenomenon will be occurred and extra conduction electrons will be formed. The resonance phenomenon in nanoparticle is occurred at the exact wavelength. In other researches, nanoparticles were introduced into optical layer of solar cells and only preliminary effect of nanoplasmonics such as nanoplasmonic-optic was used to enhance optical properties of solar cells. If metal nanoparticles are introduced into emitter region of silicon solar cell, both effects of nanoplasmonics can be used effectively. Since, formed hot electrons owing to resonance phenomenon in nanoparticles can participate in carriers transport and affect to recombination processes. Hence, in this paper, we decided to input the gold nanoparticles into emitter region of silicon solar cell. Besides, physical properties of gold nanoparticles with various sizes were collected from experimental sources to increase reliability of simulation. In addition, we studied the influence of size of gold nanoparticle on properties of silicon solar cell owing to strongly depending of optical and electrical properties of gold nanoparticles on their sizes.

Method

Mainly, three methods are used to explore solar cells. They are theory, experiment and simulation. In this paper, simulation method is utilized to study influence of gold nanoparticles on properties of silicon solar cell. Sentaurus TCAD (Technology Computing Aided Design) has been used for simulation. There are a lot of instruments in Sentaurus TCAD but only four of them have been utilized in this study. They are Sentaurus Structure Editor, Sentaurus Device, Sentaurus Visual and Sentaurus Workbench. Each instrument has own task. In Sentaurus Structure Editor, the geometric models of gold nanoparticles with various sizes introduced silicon solar cells have been created. In our previous works, we wrote about creating the geometric models of solar cells by using Tool Command Language in Sentaurus Structure Editor [29]. In fig. 1, geometric structure of nanoparticles introduced silicon solar cells is shown. So, nanoparticles are introduced into n region. In Sentaurus Device, physical properties are given to geometric model and perform calculation by using numerical method. In Sentaurus Visual, obtained results are generated with visual or graphical form, in order to analyze them. Sentaurus Workbench help the above three instruments to work together simultaneously.

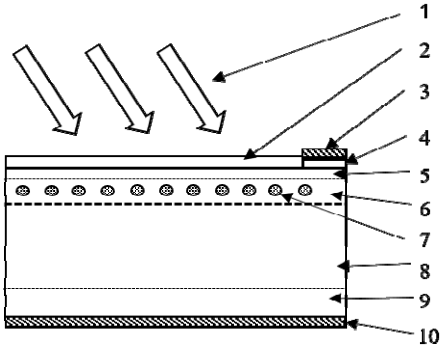

Fig. 1. Nanoparticles introduced silicon solar cell. 1 – light, 2 – antireflection coating, 3 – front contact, 4 – contact region, 5 – n++ region, 6 – n region, 7 – nanoparticles, 8 – p region, 9 – p++ region and 10 – rear contact

Materials properties in Sentaurus material database is for bulk materials not nanoscale materials. But, in Sentaurus TCAD the physical properties of materials can be changed by editing the parameter files. So, it is allowed to change the material properties in Sentaurus Device. When the size of materials is decreased up to nanoscale, quantum size effects begin to appear. Thus, in nanoscale, properties of materials will be variously depended on their size. Because, the number of atoms is decreased significantly. In this paper, dependence of refractive index and work function of metal nanoparticles on their sizes is used to study the influence of gold nanoparticles on optic and electric properties of silicon solar cell. Refractive index data of gold nanoparticles with size of 4 nm, 6 nm, and 9 nm were taken from Yakubovskiy's experimental works [30]. For the size of 11 nm and 21 nm, data were

taken from Rosenblatt's researches [31]. In fig. 2, dependence of the real (a) and imaginary part (b) of complex refractive index of gold nanoparticles with sizes of 4 nm and 21 nm on wavelength is described. Real part of complex refractive index of gold nanoparticles with size of 4 nm has been greater than that of gold nanoparticle with size of 21 nm but imaginary part has been lower. In Khao's ultraviolet photoelectron spectroscopic analysis, it was found that decreasing of work function of gold nanoparticles from 5.76 eV to 5.36 eV when size of nanoparticles was changed from 40 nm to 5 nm [32]. In modeling, five parameter files have been created for gold nanoparticles with sizes of 4 nm, 6 nm, 9 nm, 11 nm, 21 nm. Physical properties were written into parameter files respectively each size of gold nanoparticles.

Uploading the parameters files, which includes physical properties with suitable size of nanoparticle, was performed with Sentaurus Workbench.

In Sentaurus Device, numerical methods are used to simulate semiconductor devices. Therefore, geometric models are meshed to acceptable sizes. Active regions of solar cells are meshed with smaller sizes and passive regions are meshed with greater sizes. For instance, in this paper, whole AuNISSC has been meshed with size of 0.005 μm and p-n junction, contact, and nanoparticles located regions are meshed with size of 0.001 μm.

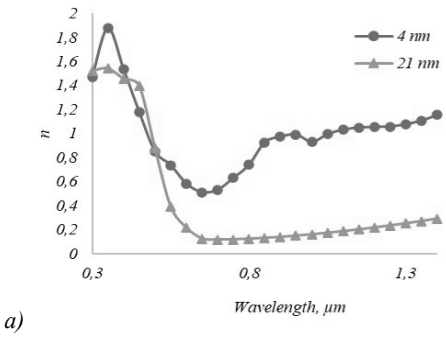

a)

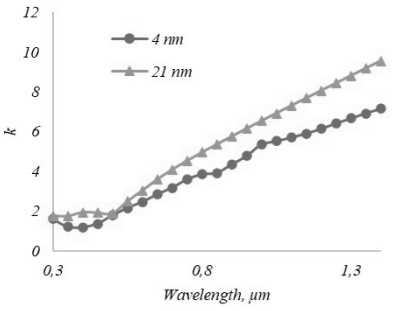

b)

Fig. 2. Dependence of real (a) and imaginary (b) parts of complex refractive indices of gold nanoparticles with size of 4 nm and 21 nm on wavelength

Experimental obtained physical parameters of materials and fundamental physical theory of numerical methods are base of each performed simulations. If carriers in semiconductor devices is equilibrium state, calculating the Poisson equation [33] shown in equation (1) will be enough to determine their electrical parameters.

$$\Delta\varphi = -\frac{q}{\varepsilon}\left(p - n + N_D + N_A\right). \quad (1)$$

Where: ε is permittivity, n and p are concentration of electron and holes, N_D and N_A are concentration of donor and acceptor, q is electron charge.

Electron (n) and holes (p) concentration, which are used in Poisson equation, are calculated by using Fermi statistic that are given equation (2) and (3).

$$n = N_c F_{1/2}\left(\frac{E_{F,n} - E_c}{kT}\right), \quad (2)$$

$$p = N_V F_{1/2}\left(\frac{E_V - E_{F,p}}{kT}\right). \quad (3)$$

Where: $F_{1/2}$ is Fermi half integral, E_c is conduction band energy, E_v is valence band energy, $E_{F,n}$ is quasi fermi energy for electrons, $E_{F,p}$ is quasi fermi energy for holes, T is absolute temperature, N_c is density of states in conduction band, N_v is density of states in valence band, k is Boltzmann constant.

Due to the fact that solar cells are optoelectronic device, studying of physical parameters of the solar cells is more difficult than other semiconductor devices. Simulation of solar cells is divided into two main parts that are optic and electric. First, the optical properties of solar cell are determined. In this paper, Transfer Matrix Method (TMM) shown equation (4) was used to calculate optic parameters of AuNISSCs. Because, TMM can take into account interference phenomenon. In TMM, fresnel formulas shown equation (5) and (6) has been utilized to define optical boundary conditions.

$$\begin{bmatrix} E_i \\ E_2 \end{bmatrix} = M \begin{bmatrix} E_t \\ 0 \end{bmatrix}. \quad (4)$$

$$\begin{cases} r_\perp = \dfrac{n_1 \cos\alpha - n_2 \cos\gamma}{n_1 \cos\alpha + n_2 \cos\gamma} \\ t_\perp = \dfrac{2n_1 \cos\alpha}{n_1 \cos\alpha + n_2 \cos\gamma} \end{cases}, \quad (5)$$

$$\begin{cases} r_\parallel = \dfrac{n_1 \cos\gamma - n_2 \cos\beta}{n_1 \cos\gamma + n_2 \cos\beta} \\ t_\parallel = \dfrac{2n_1 \cos\beta}{n_2 \cos\beta + n_1 \cos\gamma} \end{cases}, \quad (6)$$

where: M is transfer matrix, E_i is the electric field of the incident light, E_r is the electric field of the reflected light, E_t is the electric field of the transmitted light, n_1 and n_2 are the refractive indices of mediums; β is the angle of incident light; γ is the angle of refracted light; r and t are the Fresnel coefficients.

After illuminating the solar cells, the electron-holes generate, potential difference between contacts and carriers transport form. Carrier transport will be caused the changing the carrier concentration and it forms current. Connection between the changing carrier concentration, which is in volume of device, and current is expressed by using the continuity equation which is given equation (7) and (8).

$$\nabla \cdot \vec{J}_n = qR_{net,n} + q\frac{\partial n}{\partial t}. \quad (7)$$

$$-\nabla \vec{J}_p = qR_{net,p} + q\frac{\partial p}{\partial t}. \quad (8)$$

Where: J_n, J_p are the current densities of electron and holes, $R_{net,p}$, $R_{net,n}$ are the net recombination of electron and holes, t – time

Due to metal nanoparticles introduced into silicon solar cell, "Thermodynamic" model is used to calculate carrier transport. Because, "Thermodynamic model" can take into account influence of external heat, which was formed around the nanoparticles due to oscillation of free electrons on the surface of nanoparticles. Besides, in addition to minority and majority carriers transport, it can also calculate transport of external carriers, which was formed due to resonance phenomenon in the nanoparticles. In "Thermodynamic" model, transports of electron and holes in semiconductor are calculated by using equation (9) and (10).

$$\vec{J}_n = -nq\mu_n(\nabla \Phi_n + P_n \nabla T). \quad (9)$$

$$\vec{J}_p = -pq\mu_p(\nabla \Phi_p + P_p \nabla T). \quad (10)$$

Where: μ_n, μ_p are mobility of electron and holes, Φ_n, Φ_p are the electron and hole quasi-Fermi potentials, P_n, P_p are thermoelectric power of electron and holes, T is absolute temperature.

Transport of carriers in the metal distinguish from transport in semiconductors. Therefore, another equation (11) of "Thermodynamic" model, was used to calculate the transport of electrons in gold nanoparticles.

$$\vec{J}_M = -\sigma(\nabla \Phi_M + P\nabla T). \quad (11)$$

Where: σ is conductivity of metal, Φ_m is Fermi potential in metal, P is the metal thermoelectric power, J_M is current density in the metal.

There is ohmic boundary condition between gold nanoparticle and n type silicon. Therefore, ohmic boundary condition, which is given equation (9), is used to identify the distribution of carriers and current between gold nanoparticle as well as n type silicon.

$$\begin{aligned} &\vec{J}_M \cdot \hat{n} = (\vec{J}_n + \vec{J}_p + \vec{J}_D) \cdot \hat{n}, \\ &\varphi = \Phi_M - \Phi_0, \\ &n = n_0, \\ &p = p_0. \end{aligned} \quad (12)$$

Where: J_D is diffusion current density, $\hat{n}$ is normal vector, Φ_0 is the equilibrium electrostatic potential (the built-in potential), ϕ – electrostatic potential, n_0, p_0 are the electron and hole equilibrium concentrations.

Results and discussion

First, geometrical models of AuNISSCs with nanoparticle size of 4 nm, 6 nm, 9 nm, 11 nm and 21 nm have been created in Sentaurus TCAD by using algorithm created with Tool Command Language. AuNISSC was consist of six layers with various thicknesses. They were 60 nm SiO_2, 90 nm high doped n-type silicon, 150 nm emitter, 1080 nm base and 120 nm high doped p-type silicon. Concentration of phosphorous atoms was 1e18 cm^{-3} in high doped n-type silicon layer and 1e17 cm^{-3} in emitter layer. Concentration of Bohr atoms was 1e15 cm^{-3} in base and 1e16 cm^{-3} in high doped p-type silicon layer. In fig. 3, dependence of open circuit voltage of AuNISSC on size of Au nanoparticle is shown. When size of nanoparticle was increased from 4 nm to 11 nm, open circuit voltage didn't change from 0.498 V. But, when size of nanoparticle was increased to 21 nm, open circuit voltage dropped to 0.481 V. Open circuit voltage strongly depend on recombination processes. That's why, rear side of silicon solar cells is covered with surface passivation coating to improve the open circuit voltage [34]. In our point of view, high energy electrons formed in nanoparticles converts one part of their energy to heat energy then form phonons as well as their energy equal to conduction band energy of n-type silicon then they move in silicon as conduction electrons. Formed phonons can cause the reducing of open circuit voltage as obtained in our simulation results. When size of nanoparticles was increased, reducing of open circuit voltage was observed in Reineck's experiments [35]. Besides, when nanoplasmonic effect occur in volume of silicon, heat flux generated and temperature of solar cells changed due to Fano resonance then it causes dropping of open circuit voltage. When a metal nanoparticle is illuminated, part of the intercepted light is scattered in the surroundings, while the other part gets absorbed and ultimately dissipated into heat [36].

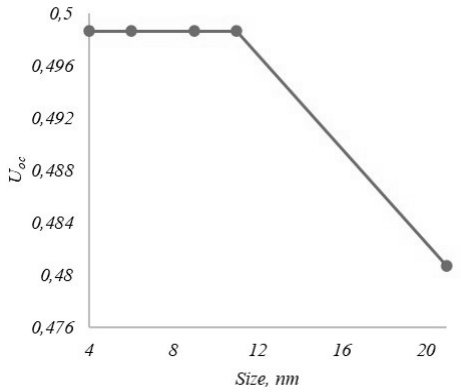

Fig. 3. Dependence of open circuit voltage of gold nanoparticle introduced silicon solar cell on radius of nanoparticles

If energy of incident photons on the surface of solar cell is high from or equal to band gap energy, they are absorbed and generate electron-hole pairs. Transport of all generated electron-hole pairs form photocurrent. Part of generated carriers due to photogeneration recombine until they reach the contacts and this part of carriers form the recombination current. If recombination current is subtracted from photocurrent, short circuit current is gotten. So, only electrons that are reached to contacts form short circuit current. In fig. 4, dependence of short circuit cur-

rent of AuNISSC on nanoparticle size is shown. When size of gold nanoparticle was increased from 4 nm to 9 nm, short circuit current dropped from 6.5 mA / cm^2 to 6 mA / cm^2. Short circuit current gained its maximum value 6.7 mA / cm^2, when nanoparticle size was 11 nm. When nanoparticle size was increased up to 21 nm, short circuit current gained its minimum value of 3.1 mA / cm^2. In Chander's experiments, it was observed alike our results that short circuit current of dye-sensitized solar cell, which included gold nanoparticles, increased and decreased like a wave when size of nanoparticle was increased [37]. Ratio of energies of nanoparticle absorbed and scattered light depend on light wavelength and size of nanoparticle [38]. Therefore, in our results, the short circuit current also changed depend on the size of nanoparticle. In Reineck's experiment on the AuNISSC, short circuit current decrease by 26 % when size of nanoparticles increased from 10 nm to 20 nm [39]. Short circuit current strongly depends on light intensity or number of absorbed photons. In Mie theory of plasmonics, light, incident light on metal nanoparticles divided three part that are extinction, scattering and absorption. When size of nanoparticles changed, ratio of parts change. Scattering light help to increase short circuit current of solar cell owing to wavelength of scattered light is very close to silicon absorption spectrum. Besides, absorbed photons concentration in silicon can increase when scattered photons from metal nanoparticles is absorbed.

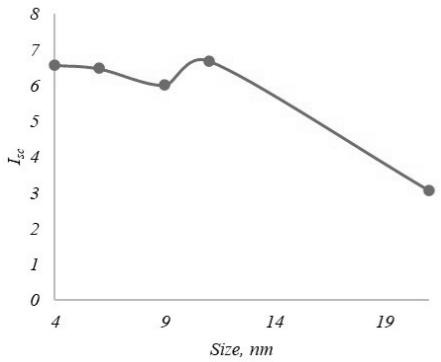

Fig. 4. Dependence of short circuit current of NISSC on size of nanoparticles

In figure 5, dependence of fill factor of AuNISSC on size of nanoparticles is described. In this paper, curve of fill factor is almost like curve of short circuit current. But, maximum value of fill factor was observed at the nanoparticle size of 4 nm. When size of nanoparticle was increased from 4 nm to 9 nm, fill factor decreased by 0.59 %. When size of nanoparticle was increased from 9 nm to 11 nm, fill factor increased by 0.44 %. When size of nanoparticle was increased from 11 nm to 21 nm, fill factor decreased by 1.25 %. Fill factor is indication of quality of solar cell and it strongly depends on series resistivity of solar cell and recombination rate. Due to nanoparticles was introduced into emitter region of silicon solar cell, it affected the total resistivity and recombination rate of emitter region. If total resistivity of emitter consists of addition of resistivities of gold nanoparticles and n-type silicon and total resistivity will directly depend on ratio of their volume. But, Chander introduced gold nanoparticles into TiO_2 layer of dye-sensitized and he observed that fill factor increased when nanoparticles size was enlarged [37].

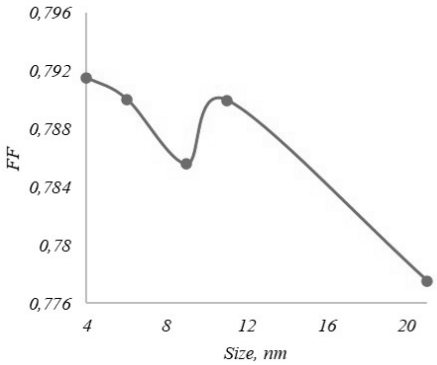

Fig. 5. Dependence of fill factor of NISSC on radius of nanoparticles

Main photoelectric parameters of solar cells are determined by using I-V characteristics. Curves, which is shown in above fig. 4, 5, and 6, were generated by determining the I-V characteristics of AuNISSCs, which consist nanoparticles with sizes of 4 nm, 6 nm, 9 nm, 11 nm, and 21 nm. It was found from obtained results that fill factor gain its maximum value at nanoparticles size of 11 nm and minimum value at nanoparticles size of 21 nm. Therefore, in fig. 6, I-V characteristics of those are described. So, figure 6 shows that if nanoprticels size is increased from 11 nm to 21 nm, the I-V characteristics are getting deteriorated. In Notarian's experiment like our results, deterioration of I-V characteristics of AuNISSC was observed when size of nanoparticles was increased [40]. In this paper, when gold nanoparticles with size of 11 nm was introduced into emitter region of silicon solar cell, they increased efficiency of silicon solar cell by 1.7 %. Pudasini found by using numerical simulation that efficiency of silicon solar cell increased by 25.42 % after introducing gold nanoparticles [41]. Because, he used SiO_2 / SiN_x double antireflection coatings to enhance optical properties and passivate the surface. Besides, he used silicon with nanoholes. But, Narges found in his experiment that when gold nanoparticles were introduced into traditional wafer based multi-crystalline silicon solar cell, efficiency of that solar cell increased by 1.97 % [42]. So, our simulation results are more suitable to Narges's experimental results and it proves reliability of our simulation results.

Reason for changing the photoelectric parameters after introducing of nanoparticles is altering of absorption coefficient due to nanoplasmonic effect. Because, in nanoplasmonic effect metal nanoparticles absorb light with long wavelength and emit lights with short wavelength owing to Mie scattering. Nanoplasmoci effect is ex-

plained by Mie scattering. Thus, in fig. 7, spectral characteristics of absorption coefficients of silicon solar cell without nanoparticles, and AuNISSCs, which consist of nanoparticles with size of 4 nm and 21 nm, is described. Absorption coefficient of silicon solar cell without nanoparticles gain its maximum value at wavelength of 435 nm. In wavelength of over the 450 nm, absorption coefficient of silicon solar cell without nanoparticles dropped exponentially. It was found from also our obtained spectral characteristics like spectral characteristics of silicon solar cell given in other reference [43] that silicon solar cell mainly absorbs light in visible spectrum. Spectral characteristics changed significantly after introducing the gold nanoparticles. Absorption coefficient of AuNISSC, which consists of gold nanoparticles with size of 11 nm, increased in infra-red spectrum. Reason for forming the waves in range of wavelength between 400 nm and 560 nm is light interference of electromagnetic waves, which is emitted from nanoparticles. Therefore, AuNISSC can absorb infrared light. Our results is suitable to Joseph's work [44]. Gold nanoparticle absorbs the light in infrared spectrum and emits light that silicon can absorb. When size of nanoparticle was decreased, wavelength of maximum of absorption coefficient in spectrum increased by 10 nm. In spectrum of absorption coefficient, maximum and minimum values belong to interference maxima and minima. This phenomenon is called Fano interference [45].

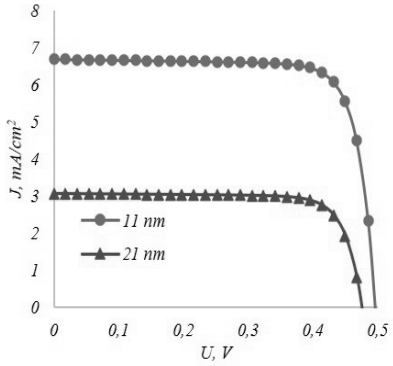

Fig. 6. I-V characteristics of gold nanoparticles with size of 11 nm and 21 nm introduced silicon solar cell

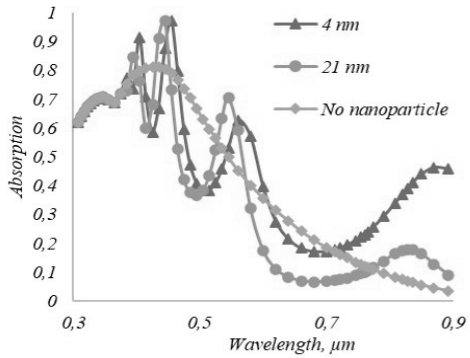

Fig. 7. Dependence of absorption coefficient of silicon solar cell without nanoparticles, and AuNISSC, which consist of nanoparticles with sizes of 4 nm and 21 nm, on wavelength

One of the main losses in thin film silicon solar cells is high value of transmission coefficient. In figure 8, distribution of absorbed photon density for silicon solar cell without nanoparticles, and AuNISSC, which consist of nanoparticles with size of 11 nm, is described. In silicon solar cell without nanoparticles, absorption photons density decreased exponentially through thickness of solar cell like other researcher's result [46]. After introducing the gold nanoparticles, absorption in nanoparticles introduced region increased significantly due to nanoplasmonic effect [47]. Therefore, in Atwater's researches, it was found that thickness of silicon solar cell can be smaller than 2 μm and greater than 100 nm due to plasmonic effect [48].

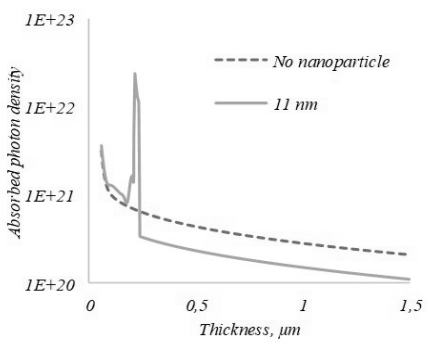

Fig. 8. Distribution of absorbed photon density through thickness of Au NISSC and SSC

Conclusion

In this paper, gold nanoparticles with various sizes have been introduced into emitter region of silicon solar cell. Shifting of resonance of absorption spectrum was observed when nanoparticles size changed. So, in experiments, size of nanoparticles, which are introduced into silicon solar cell, can be identified by analyzing absorption spectrum. In the future, this idea will help to conduct experiments. It was found that influence of gold nanoparticles on electrical properties such as resistivity and recombination of solar cell was noticeable. When size of gold nanoparticles was enlarged from 11 nm to 21 nm, I-V characteristics deteriorated sharply. Therefore, size of introduced nanoparticles is important. It was found that most acceptable size of gold nanoparticles for silicon solar cell is 11 nm. Sharply increasing of absorption coefficient in nanoparticles introduced region was observed when distribution of absorbed photon density across the thickness of AuNISSC was calculated. Reducing the thickness of the silicon-based solar cell without changing the efficiency at the same time can be achieved. So, cost of silicon solar cell can be reduced. Due to gold nanoparticles were introduced into emitter region of silicon solar cell, nanoplasmonic-electric and nanoplasmonic-optic effects were occurred at the same time. It was found that role of nanoplasmonic-optic effect in changing the photoelectric parameters of silicon solar cell is greater than nanoplasmonic-electric effect due to nanoparticles affected more noticeable to short circuit current than open circuit voltage.

References

[1] Meyer AR, et al. Atomic structure of light-induced efficiency-degrading defects in boron-doped Czochralski silicon solar cells. Energy Environ Sci 2021; 14(10): 5416-5422. DOI: 10.1039/d1ee01788h.

[2] Xiang HJ, Huang B, Kan E, Wei SH, Gong XG. Towards direct-gap silicon phases by the inverse band structure design approach. Phys Rev Lett 2013; 110(11): 118702. DOI: 10.1103/PhysRevLett.110.118702.

[3] Gu YQ, Xue CR, Zheng ML. Technologies to reduce optical losses of silicon solar cells. Adv Mat Res 2014; 953-954: 91-94. DOI: 10.4028/www.scientific.net/AMR.953-954.91.

[4] Saravanan S, Dubey RS, Kalainathan S, More MA, Gautam D K. Design and optimization of ultrathin crystalline silicon solar cells using an efficient back reflector. AIP Adv 2015; 5(5): 057160. DOI: 10.1063/1.4921944.

[5] Huang X, Han S, Huang W, Liu X. Enhancing solar cell efficiency: the search for luminescent materials as spectral converters. Chem Soc Rev 2012; 42(1): 173-201. DOI: 10.1039/C2CS35288E.

[6] Lopez-Delgado R, et al. Enhanced conversion efficiency in Si solar cells employing photoluminescent down-shifting CdSe/CdS core/shell quantum dots. Sci Rep 2017; 7(1): 14104. DOI: 10.1038/s41598-017-14269-0.

[7] Trupke T, Green MA, Würfel P. Improving solar cell efficiencies by down-conversion of high-energy photons. J Appl Phys2002; 92(3): 1668. DOI: 10.1063/1.1492021.

[8] Richards BS. Enhancing the performance of silicon solar cells via the application of passive luminescence conversion layers. Sol Energy Mater Sol Cells 2006; 90(15): 2329-2337. DOI: 10.1016/j.solmat.2006.03.035.

[9] Klampaftis E, Ross D, McIntosh KR, Richards BS. Enhancing the performance of solar cells via luminescent down-shifting of the incident spectrum: A review. Sol Energy Mater Sol Cells 2009; 93(8): 1182-1194. DOI: 10.1016/j.solmat.2009.02.020.

[10] van Sark WGJHM, de Wild J, Rath JK, Meijerink A, Schropp REI. Upconversion in solar cells. Nanoscale Res Lett 2013; 8(1): 81. DOI: 10.1186/1556-276X-8-81.

[11] Kumaragurubaran B, Anandhi S. Reduction of reflection losses in solar cell using Anti Reflective coating. 2014 Int Conf on Computation of Power, Energy, Information and Communication (ICCPEIC 2014) 2014: 155-157. DOI: 10.1109/ICCPEIC.2014.6915357.

[12] Kim J. Optimization of SiNx layer for solar cell using computational method. Curr Appl Phys 2011; 11(1): S39-S42. DOI: 10.1016/j.cap.2010.11.048.

[13] Glunz SW, Feldmann F. SiO2 surface passivation layers – a key technology for silicon solar cells. Sol Energy Mater Sol Cells 2018; 185: 260-269. DOI: 10.1016/j.solmat.2018.04.029.

[14] S. Y. Lien, D. S. Wuu, W. C. Yeh, and J. C. Liu, "Tri-layer antireflection coatings (SiO2/SiO2–TiO2/TiO2) for silicon solar cells using a sol–gel technique," Sol Energy Mater Sol Cells 2006; 90(16): 2710-2719. DOI: 10.1016/j.solmat.2006.04.001.

[15] Gulomov J, Aliev R. Analyzing periodical textured silicon solar cells by the TCAD modeling. Sci Tech J Inf Technol Mech Opt 2021; 21(5): 626-632. DOI: 10.17586/2226-1494-2021-21-5-626-632.

[16] Han SE, Chen G. Optical absorption enhancement in silicon nanohole arrays for solar photovoltaics. Nano Lett 2010; 10(3): 1012-1015. DOI: 10.1021/NL904187M.

[17] Al-Ashouri A, et al. Monolithic perovskite/silicon tandem solar cell with >29% efficiency by enhanced hole extraction. Science 1979; 370(6522): 1300-1309. DOI: 10.1126/science.abd4016.

[18] Khokhar MQ, et al. High-efficiency hybrid solar cell with a nano-crystalline silicon oxide layer as an electron-selective contact. Energy Convers Manag 2022; 252: 115033. DOI: 10.1016/j.enconman.2021.115033.

[19] Kadhum HA, Salih WM, Rheima AM. Improved PSi/c-Si and Ga/PSi/c-Si nanostructures dependent solar cell efficiency. Appl Phys A 2020; 126(10): 802. DOI: 10.1007/s00339-020-03985-6.

[20] Yalamanchili S, Lewis NS, Atwater HA. Role of doping dependent radiative and non-radiative recombination in determining the limiting efficiencies of silicon solar cells. 2018 IEEE 7th World Conf on Photovoltaic Energy Conversion, WCPEC 2018 – A Joint Conf of 45th IEEE PVSC, 28th PVSEC and 34th EU PVSEC 2018: 3223-3226. DOI: 10.1109/PVSC.2018.8547758.

[21] Pang SK, Smith AW, Rohatgi A. Effect of trap location and trap-assisted auger recombination on silicon solar cell performance. IEEE Trans Electron Devices 1995; 42(4): 662-668. DOI: 10.1109/16.372065.

[22] Gogolin R, Harder NP. Trapping behavior of Shockley-Read-Hall recombination centers in silicon solar cells. J Appl Phys 2013; 114(6): 064504. DOI: 10.1063/1.4817910.

[23] Choy WCH. Plasmon-optical and plasmon-electrical effects for improve performances of solar cells. 2016 Progress in Electromagnetic Research Symposium (PIERS) 2016: 1686-1686. DOI: 10.1109/PIERS.2016.7734762.

[24] Castelletto S, Boretti A. Noble metal nanoparticles in thin film solar cells. Nanosci Nanotechnol Lett 2013; 5(1): 36-40. DOI: 10.1166/NNL.2013.1396.

[25] Gulomov J, et al. Studying the effect of light incidence angle on photoelectric parameters of solar cells by simulation. Int J Renew Energy Dev 2021; 10(4): 731-736. DOI: 10.14710/ijred.2021.36277.

[26] Zhang JJ, Qu ZG, Zhang JF, Maharjan A. A three-dimensional numerical study of coupled photothermal and photoelectrical processes for plasmonic solar cells with nanoparticles. Renew Energy 2021; 165: 278-287. DOI: 10.1016/j.renene.2020.11.010.

[27] Eremin YA, Lopushenko VV. Numerical analysis of the functional properties of the 3D resonator of a plasmon nanolaser with regard to nonlocality and prism presence via the discrete sources method. Computer Optics 2021; 45(3): 331-339. DOI: 10.18287/2412-6179-CO-790.

[28] Butt MA, Khonina SN, Kazanskiy NL. An array of nanodots loaded MIM square ring resonator with enhanced sensitivity at NIR wavelength range. Optik 2020; 202: 163655. DOI: 10.1016/j.ijleo.2019.163655.

[29] Abduvohidov MK, Aliev R, Gulomov J. A study of the influence of the base thickness on photoelectric parameters of silicon solar cells with the new TCAD algorithms. Scientific and Technical Journal of Information Technologies, Mechanics and Optics 2021; 21(5): 774-784. DOI: 10.17586/2226-1494-2021-21-5-774-784.

[30] Yakubovsky DI, et al. Ultrathin and ultrasmooth gold films on monolayer MoS2. Adv Mater Interfaces 2019; 6(13): 1900196. DOI: 10.1002/ADMI.201900196.

[31] Rosenblatt G, Simkhovich B, Bartal G, Orenstein M. Nonmodal plasmonics: Controlling the forced optical response of nanostructures. Phys Rev X 2020; 10(1): 011071. DOI: 10.1103/PhysRevX.10.011071.

[32] Khoa NT, Kim SW, Yoo DH, Kim EJ, Hahn SH. Size-dependent work function and catalytic performance of gold nanoparticles decorated graphene oxide sheets. Appl Catal A-Gen 2014; 469: 159-164. DOI: 10.1016/j.apcata.2013.08.046.

[33] Devi LB, et al. A numerical simulation and modeling of poisson equation for solar cell in 2 dimensions. IOP Conference Series: Earth and Environmental Science 2018; 173(1): 012001. DOI: 10.1088/1755-1315/173/1/012001.
[34] Stem N, Ramos CAS, Cid M. Open-circuit voltages: Theoretical and experimental optimizations of rear passivated silicon solar cells using Fz and Cz wafers. Solid State Electron 2010; 54(3): 221-225. DOI: 10.1016/j.sse.2009.09.002.
[35] Reineck P, Brick D, Mulvaney P, Bach U. Plasmonic hot electron solar cells: The effect of nanoparticle size on quantum efficiency. J Phys Chem Lett 2016; 7(20): 4137-4141. DOI: 10.1021/acs.jpclett.6b01884.
[36] Baffou G, Quidant R, Girard C. Heat generation in plasmonic nanostructures: Influence of morphology. Appl Phys Lett 2009; 94(15): 153109. DOI: 10.1063/1.3116645.
[37] Chander N, et al. Size and concentration effects of gold nanoparticles on optical and electrical properties of plasmonic dye sensitized solar cells. Solar Energy 2014; 109: 11-23. DOI: 10.1016/j.solener.2014.08.011.
[38] Wang L, Kafshgari MH, Meunier M. Optical properties and applications of plasmonic-metal nanoparticles. Adv Funct Mater 2020; 30(51): 2005400. DOI: 10.1002/adfm.202005400.
[39] Reineck P, Brick D, Mulvaney P, Bach U. Plasmonic hot electron solar cells: the effect of nanoparticle size on quantum efficiency. J Phys Chem Lett 2016; 7(20): 4137-4141. DOI: 10.1021/acs.jpclett.6b01884.
[40] Notarianni M, Vernon K, Chou A, Aljada M, Liu J, Motta N. Plasmonic effect of gold nanoparticles in organic solar cells. Solar Energy 2014; 106: 23-37. DOI: 10.1016/j.solener.2013.09.026.
[41] Pudasaini PR, Ayon AA. Nanostructured thin film silicon solar cells efficiency improvement using gold nanoparticles. Phys Status Solidi A 2012; 209(8): 1475-1480. DOI: 10.1002/pssa.201228022.
[42] Jia B, Gu M, Fahim N, Zhang Y, Shi Z, Ouyang Z. Efficiency enhancement of screen-printed multicrystalline silicon solar cells by integrating gold nanoparticles via a dip coating process. Opt Mater Express 2012; 2(2): 190-204. DOI: 10.1364/OME.2.000190.
[43] Bläsi B, Rüdiger M, Peters M, Platzer W. Electro – optical simulation of diffraction in solar cells. Opt Express 2010; 18(S4): A584-A593. DOI: 10.1364/OE.18.00A584.
[44] Day J, Senthilarasu S, Mallick TK. Improving spectral modification for applications in solar cells: A review. Renew Energy 2019; 132: 186-205. DOI: 10.1016/j.renene.2018.07.101.
[45] Lombardi A, et al. Fano interference in the optical absorption of an individual gold-silver nanodimer. Nano Lett 2016; 16(10): 6311-6316. DOI: 10.1021/acs.nanolett.6b02680.
[46] Ghosh H, et al. Light-harvesting properties of embedded tin oxide nanoparticles for partial rear contact silicon solar cells. Plasmonics 2016; 12(6): 1761-1772. DOI: 10.1007/S11468-016-0443-7.
[47] Hossain MK, Mukhaimer AW, Drmosh QA. Spectral absorption depth profile: A step forward to plasmonic solar cell design. J Electron Mater 2016; 45(11): 5695-5702. DOI: 10.1007/S11664-016-4808-7.
[48] Atwater HA, Polman A. Plasmonics for improved photovoltaic devices. Nat Mater 2010; 9(3): 205-213. DOI: 10.1038/nmat2629.

Authors' information

Jasurbek Gulomov (b. 1999) graduated from Andijan State University named after Z.M.Bobur in 2021, majoring in Physics. Currently he works as the researcher at the Renewable Energy Sources Laboratory of Andijan State University. Besides, now, he is master student of Physics of renewable energy sources and sustainable environment at the Andijan State University. Research interests are numerical simulation, nanoplasmonic solar cells, metal nanoparticles and programming. E-mail: *jasurbekgulomov@yahoo.com* .

Rayimjon Aliev, (b. 1958), graduated from Andijan State University named after Z.M.Bobur in 1979, majoring in Physics. Currently, he is professor of Physics department of Andijan State University and head of Renewable Energy Sources Laboratory. Research interests: solar cells, nanoplasmonics, simulation, nanostructured solar cells, silicon, textures, antireflection coatings, hybrid solar-wind and solar-hydro energy sources. E-mail: *alievuz@yahoo.com* .

Irodakhon Gulomova (b. 1999) is studying at Andijan State University named after Z.M.Bobur in 2021, majoring in Physics. Currently She works as the researcher at the Renewable Energy Sources Laboratory of Andijan State University. Research interests are TCAD simulation, programming, and solar cells. E-mail: *suntulip2612@gmail.com* .

Received December 16, 2021. The final version – May 19, 2022.